

# EXPERIMENTAL AND ANALYTICAL STUDY OF A NEW KIND OF STEEL-PVA HYBRID FIBER CONCRETE IN THE ANCHORAGE ZONE OF A BRIDGE EXPANSION AND CONTRACTION INSTALLATION

## EKSPERIMENTALNA IN ANALITIČNA ŠTUDIJA NOVE VRSTE HIBRIDNEGA BETONA IZ JEKLA IN PVA VLAKEN ZA SIDRIŠČE INŠTALACIJE RAZTEZANJA IN KRČENJA MOSTU

Minshui Huang<sup>1\*</sup>, Zihao Wan<sup>1</sup>, Yongzhi Lei<sup>1</sup>, Xin Shi<sup>2</sup>, Guoming Shu<sup>2</sup>

<sup>1</sup>School of Civil Engineering and Architecture, Wuhan Institute of Technology, 693 Xiongchu Ave., Wuhan 430073, Hubei, China

<sup>2</sup>Department of Civil Engineering, Hebei Jiaotong Vocational and Technical College, 219 Pearl River Avenue, Yuhua, Shijiazhuang 050035, Hebei, China

*Prejem rokopisa – received: 2020-04-02; sprejem za objavo – accepted for publication: 2020-11-13*

doi:10.17222/mit.2020.053

In this paper, a new kind of steel-polyvinyl alcohol (PVA) hybrid fiber concrete with high early strength and better road performance is proposed for use in the anchorage zone of a bridge expansion and contraction installation (BECI). Firstly, a comprehensive test design method is adopted to evaluate the mechanical properties of the concrete by adding different percentages of fibers, and the optimal percentages of steel and PVA fiber additives are determined. The results of the compressive and flexural strength test indicated that the concrete with added 1.5 % steel fiber and 0.12 % PVA fiber has a higher early strength. Secondly, to evaluate the performance of the improved concrete, the finite-element method was adopted to model the anchorage zone concrete of the BECI, and the loading location of maximum stress was determined and some factors, such as overload and horizontal force coefficient, were considered. The maximum stresses of the anchorage zone are less than the ultimate stresses of the steel-PVA hybrid fiber concrete. It can be concluded that the improved concrete has better road performance. Finally, a case study of the actual bridge was carried out to verify the practical value of the steel-PVA hybrid fiber concrete. Although there is some reduction in the compressive strength, the new concrete is more suitable than the conventional concrete to meet the requirements for the construction of concrete in the anchorage zone of the BECI, which can reduce the construction period and show great practical application value.

**Keywords:** steel-PVA hybrid fiber concrete, bridge expansion and contraction installation, anchorage zone, finite-element method

V članku avtorji predlagajo uporabo nove vrste hibridnega betona, utrjenega z jeklenimi in polivinil alkoholnimi (PVA) vlakni, ki ima visoko začetno trdnost in boljše cestne karakteristike glede raztezanja in krčenja mostnih konstrukcij (BECI) v sidrišču oziroma vpetju. Avtorji so najprej uporabili splošno uporabljeno preizkusno metodo oblikovanja (dizajna) in določili mehanske lastnosti betona glede na različno vsebnost jeklenih in PVA-vlaknen. Rezultati preizkusov začetne tlačne in upogibne trdnosti betona so pokazali, da sta optimalni vsebnosti dodanega jekla 1,5 mas. % in 0,12 mas. % PVA-vlaknen. Sledilo je še ovrednotenje lastnosti izboljšane betona s pomočjo modela na osnovi metode končnih elementov za inštalacijo raztezanja in krčenja betonske konstrukcije v coni vpetja. S pomočjo modela so določili tudi maksimalne napetosti v tej coni in koeficient horizontalne sile. Ugotovili so, da so maksimalne sile v sidrišču manjše kot je porušna trdnost hibridnega betona vlakna iz PVA-jekla. Avtorji na osnovi izbranega primera dejanske mostne konstrukcije tudi ugotavljajo, da ima ta vrsta betona boljše cestne karakteristike. S tem so potrdili njegovo praktično vrednost oziroma uporabnost. Čeprav ima novi beton nekoliko manjšo tlačno trdnost je primernejši kot konvencionalni beton, za vpetje betonske konstrukcije ter njeno raztezanje in krčenje, kar tudi zmanjša čas izgradnje in potrjuje njegovo praktično oziroma uporabno vrednost.

**Ključne besede:** hibridni beton, ojačan z jeklom in vlakni PVA, inštalacija raztezanja in krčenja mostne konstrukcije, cona vpetja, sidrišče

## 1 INTRODUCTION

Expansion and contraction installation, a key functional part of bridges, undertakes the repeated load impact of traffic and is always exposed to adverse environmental conditions. These factors have major negative effects on the lifecycle of a BECI, which means the bridge will be easy to damage and difficult to repair. Nowadays, heavy traffic jams and economic impacts are becoming increasingly serious due to the maintenance of

BECI. But there are few researches on the rapid replacement technology of BECI. Therefore, it is critical to repair or replace the damaged BECI in a short time and overcome the problems caused by construction. Meanwhile, the durability and suitability of BECI should be ensured too.

Because the concrete in the anchorage zone has great effects on the construction period, the early mechanical properties of the concrete were studied by numerous scholars. In the early 20<sup>th</sup> century, discarded steel wire was added into concrete and used as a good additive to improve the properties of the concrete. J. P. Romualdi

\*Corresponding author's e-mail:  
huangminshui@tsinghua.org.cn (Minshui Huang)

and G. B. Baston<sup>1,2</sup> proposed a theory of fiber spacing, which is a milestone in the development of steel fiber concrete; however, the theory is for an ideal situation. The factors, such as slip between fiber and matrix concrete and uneven distribution of fiber, are not considered in the theory. The ultra-high-performance fiber concrete is introduced in 1990s to obtain the performance of high strength and toughness, and cementing material and steel fiber are both considered as good additives to ordinary concrete.<sup>3–7</sup> Fiber concrete is a composite material, which is constituted by mixing fiber with cement and mortar or matrix concrete. Compared to ordinary concrete, it has good performances of compressive strength and strain hardening. Fiber concrete can be classified into two types: single fiber and hybrid fiber. For instance, as a single fiber concrete, polyvinyl alcohol (PVA) fiber concrete has good capability of shear resistance. Its ultimate displacement in shear failure is twice more than the ordinary concrete, and its ultimate tensile strain is obviously improved.<sup>8–14</sup> Therefore, the single fiber additive can improve the mechanical properties of the concrete and durability by inhibiting its early plastic cracking and the expansion of the crack.<sup>15–17</sup>

The type, shape and size of fibers are the key factors to improve the performance of ultra-high-performance fiber concrete. Different fibers improve the performance of concrete in various ways.<sup>18–22</sup> For example, steel fiber is the main reason for strength promotion, and PVA fiber can improve the deformation capability. The experimental research of A. W. Dhawale<sup>23</sup> pointed out that PVA fiber can be used as a reinforcement additive for cementing composite material. V. C. Li<sup>24</sup> adopted PVA-engineered cementitious composites (PVA-ECC) as a rough layer of concrete to build a composited beam. The mechanical test showed that the beam has a higher ultimate strain and strength than a beam covered by plain concrete. J. S. Lawler<sup>25</sup> mixed micro PVA fiber and hook type steel fiber with mortar to make some specimens, and the flexural and shear tests proved that the bending, shearing and penetration resistance are improved. Although the single fiber additive can promote the performance of concrete, the comprehensive performance cannot satisfactorily meet the requirements of complex practical applications.

In this study, a new type of steel-PVA hybrid fiber concrete with better characteristics of high early strength, high ductility is proposed. Firstly, the comprehensive experimental method is adopted to evaluate and analyze the mechanical properties of the concrete specimens by adding different amounts of fibers, and the optimal content of steel and PVA fiber additives is determined. Furthermore the functional mechanism of the steel-PVA fiber is discussed. Then, the finite-element model of the anchorage zone concrete is setup based on ANSYS, which is exploited to comparatively evaluate the road performance of the improved concrete. Some influencing factors, such as the loading location of maxi-

um stress, the overload and horizontal force coefficient, are considered. The maximum stresses of the anchorage zone are extracted to compare with the ultimate stresses of the steel-PVA hybrid fiber concrete. Moreover, an engineering example is considered to furtherly prove the applicability of the new concrete in the maintenance of the BECI.

## 2 RAW MATERIALS AND EXPERIMENTAL METHOD

### 2.1 Raw materials

#### 2.1.1 Cement

As a key technical index that directly affects the strength value of concrete, cement plays an important role in the construction of concrete. In this study, the 42.5# general purpose Portland cement (P.O 42.5) is adopted.

#### 2.1.2 Aggregates

Aggregates can be categorized into two categories: coarse aggregate and fine aggregate. These function as the concrete framework construction and pore filling, respectively. It usually accounts for about 80 % of the concrete volume. The aggregate used in this investigation is determined according to the Chinese Standard JGJ 52.<sup>26</sup> For the coarse aggregate, the continuous graded gravel whose diameter is concentrated at the range 5–20 mm can improve the workability and avoid segregation. And for the fine aggregate, the medium sand whose diameter is concentrated at the range of 5–20 mm is selected, as shown in **Figures 1a** to **1b**.

#### 2.1.3 Water

Running water is adopted according to Chinese Standard JGJ 63.<sup>27</sup>

#### 2.1.4 Concrete admixture

The condensates of sodium naphthalene sulfonate and formaldehyde, which can be used as a water reducer, is of great physical and chemical capacity, such as water-soluble, low-foaming and stability. Its percentage of water reduction is 15 %, and the optimum mix percentage is 0.75 %. In this study, a powdered polycondensate of naphthalene sulfonate formaldehyde water-reducing agent was used, which is a brown-yellow powder in appearance. The solid content is greater than 92 %, the PH value ranges between 7 and 9, the sodium sulfate content is in the range 16–19 %. When keeping the slump unchanged, the water reduction rate varied from 12 % to 20 % (**Figure 1c**).

#### 2.1.5 Fibers

Polyvinyl alcohol (PVA) fiber and wave-shaped steel fiber, whose lengths are 6 mm and 20 mm respectively, are adopted in this study (**Figures 1d** and **1e**). The density, elongation at break, tensile strength and elastic modulus of the PVA fiber are 910 kg/m<sup>3</sup>, 17±3.0 MPa,

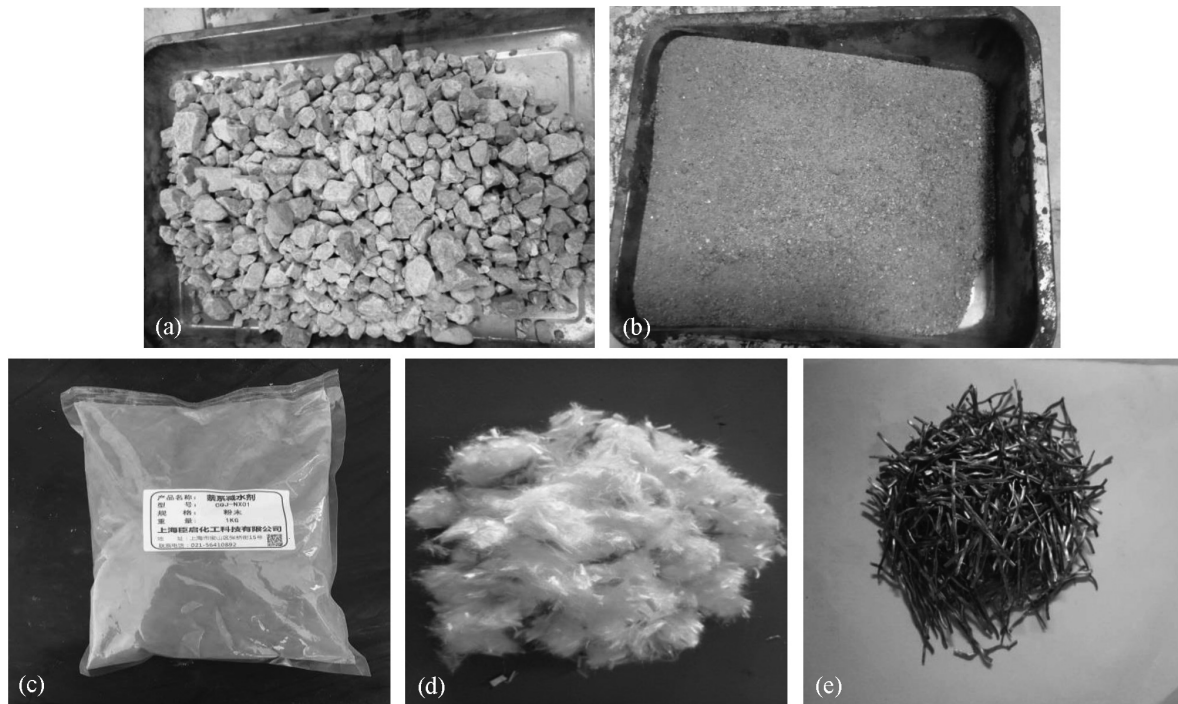


Figure 1: Raw materials: a) coarse aggregate, b) fine aggregate, c) water-reducing agent, d) PVA fiber, e) steel fiber

1400–1600 MPa and 35–39 GPa, respectively, and the corresponding parameters for the steel fiber are 7800 kg/m<sup>3</sup>, 25 MPa, 1200 MPa and 200 GPa, respectively.

## 2.2 Test design

### 2.2.1 Design of mix proportion

#### 1) Determination of the mixing strength

The strength grade design of the concrete in this paper is C50, and the mix proportion design of the concrete is carried out on this basis. The mixing strength of the concrete can be calculated as follows:

$$f_{cu,0} \geq f_{cu,k} + 1.645\sigma \quad (1)$$

where  $f_{cu,0}$  is the mixing strength of the concrete (MPa);  $f_{cu,k}$  is the standard cubic compressive strength of the concrete (MPa);  $\sigma$  is the standard deviation of the concrete strength (MPa).

The strength grade of concrete in this test is C50, so  $f_{cu,k} = 50$  MPa. For the value of  $\sigma$ , in accordance with the specification in China, JGJ55<sup>28</sup>,  $\sigma = 6$  MPa, and  $f_{cu,0} \geq 59.87$  MPa.

#### 2) Water-cement ratio

The water-cement ratio can be calculated as follows:

$$\frac{W}{B} = \frac{\alpha_a + f_{ce}}{f_{ce,0} + \alpha_a + \alpha_b + f_{ce}} \quad (2)$$

where  $W/B$  is the water-cement ratio;  $\alpha_a$  and  $\alpha_b$  are the regression coefficients, which are 0.53 and 0.20, respectively;<sup>28</sup> is the 28-days compressive strength of the mor-

tar (MPa), when the measured 28 d compressive strength of the mortar is not available, it can be determined as follows:

$$f_{ce} = \gamma_c \times f_{cu,g} = 1.16 \times 425 = 49.3 \quad (3)$$

Where  $\gamma_c$  is the surplus coefficient of the cement strength grade value, which can be determined according to the actual statistical data, and it can be selected according to JGJ55<sup>28</sup> when actual statistical data is not available;  $f_{ce,g}$  is the strength grade value of the cement (MPa).

According to Equation (2) and Equation (3), the water-cement ratio can be obtained as 0.40.

#### 3) The amount of water

The amount of water  $m_{w0}$  should comply with JGJ55.<sup>28</sup> According to the concrete slump and the graded gravel of this test, the amount of water  $m_{w0}$  is 195 kg/m<sup>3</sup>. Because the water reduction rate of the high-efficiency water reducing agent is 15 %, the amount of water is 165.75 kg/m<sup>3</sup>.

#### 4) Amount of cement and water-reducing agent

The amount of cement  $m_{b0}$  should be calculated according to Equation (4):

$$m_{b0} = \frac{m_{w0}}{W/B} = \frac{165.75}{0.4} = 414.375 \text{ kg/m}^3 \quad (4)$$

The amount of cement used is 414.375 kg/m<sup>3</sup> and the amount of water-reducing agent  $m_{a0}$  can be calculated as follows:

$$m_{a0} = m_{b0} \beta_a \quad (5)$$

Where  $\beta_a$  is the ratio of water-reducing agent (%).

5) The amount of sand and gravel

According to JGJ55,<sup>28</sup> the ratio of sand can be determined based on the type of gravel, the maximum nominal size and the water-cement ratio.

The amount of sand and gravel can be obtained as follows:

$$\begin{cases} \beta_a = \frac{m_{s0}}{m_{s0} + m_{g0}} \times 100\% \\ m_{b0} + m_{g0} + m_{s0} + m_{w0} = 2400 \end{cases} \quad (6)$$

where  $\beta_s$  is the ratio of sand (%), which is 34 % in the paper;  $m_{s0}$  is the amount of sand (kg/m<sup>3</sup>);  $m_{g0}$  is the amount of gravel (kg/m<sup>3</sup>).

The grading of the steel-PVA hybrid fiber concrete is designed according to standard specifications in China, JGJ 55<sup>28</sup> and CECS 207.<sup>29</sup> The target grade is C50, of which the actual values of cement, gravel, sand, water and water-reducing agent in the mix are (414.38, 618.79, 1201.08, 165.75 and 3.108) kg/m<sup>3</sup>, respectively.

2.2.2 Design and curing of the specimens

To obtain the mechanical behavior of the steel-PVA hybrid fiber concrete, some concrete samples were made in the laboratory. The production process of the test specimens, such as the order of feeding, the stirring method, and stirring time, can have direct or indirect effects on the overall performance of the concrete. To avoid the uneven distribution of the fibers in the tests, a dry-blending method is used to prepare the hybrid fiber concrete. The dimensions of the samples are (100×100×100) mm for compressive strength test, and (100×100×400) mm for flexural strength test. And the curing periods are 1 d and 3 d, respectively. Six sets of test specimens with a total content of 2 % and nine sets with a maximum content of 1.5 % are shown in **Table 1**.

2.3 Mechanical test

The mechanical property tests are designed according to Chinese standard, GB/T 50081,<sup>30</sup> whose main procedures of compressive strength test can be summarized as follows:

1) the test specimens at a specified age are adopted, their surfaces cleaned and the integrity checked;

2) the selected specimens are placed on the middle of the pressure plate, meanwhile, the surface which is perpendicular to the pouring surface is determined as the pressure-bearing surface (**Figure 2a**);

3) turn on the machine, when the upper-pressure plate of the machine is imminent to touch the specimen, the pressure plate stops falling and the oil return valve is closed;

4) the oil delivery valve is opened, the loading rate is limited to a constant that ranges from 0.5 MPa/s to 0.8 MPa/s;

5) when the failure of the specimen is observed and it starts to deform dramatically, adjusting the throttle of the machine is stopped until the specimen is totally broken, and the value of the failure load is recorded.

The compressive strength of concrete can be calculated as follows:

$$f_{cu,k} = \frac{F_{Cmax}}{A_C} \quad (7)$$

where  $f_{cu,k}$  is the compressive strength of the test specimen (MPa);  $F_{Cmax}$  is the ultimate loading in the compressive test (N); and  $A_C$  is the load area of test specimen (mm<sup>2</sup>).

The determination of the compressive strength should be completed with the following provisions. First, the arithmetic mean value of the measured values of the three specimens is the strength value of this group of specimens. Second, if the maximum or minimum value of the three measured values exceeds 15 % of the median value. The maximum value and the minimum value should be discarded, and the median value should be taken as the compressive strength value of this group of specimens. Third, if the maximum and the minimum values both exceed the median value by more than 15 % of the median value, the test results of this group of specimens are invalid.

When the concrete strength grade is less than C60, the strength value measured with non-standard specimens should be multiplied by the size conversion factor,

**Table 1:** Hybrid fiber content (maximum steel content is 1.5 % and total fiber content is 2 %)

Category	Maximum steel fiber content is 1.5 %			Total fiber content is 2 %		
	Specimen No.	Steel fiber	PVA	Specimen No.	Steel fiber	PVA
No fiber	S0P0	0	0	S0P0	0	0
Steel fiber only	S4P0	1	0	S2P0	2	0
	S5P0	1.5	0	/	/	/
PVA fiber only	S0P4	0	0.08	S0P2	0	2
	S0P5	0	0.12	/	/	/
Hybrid fiber	S4P4	1	0.08	S1P1	1	1
	S4P5	1	0.12	S3P1	1.5	0.5
	S5P4	1.5	0.08	S1P3	0.5	1.5
	S5P5	1.5	0.12	/	/	/

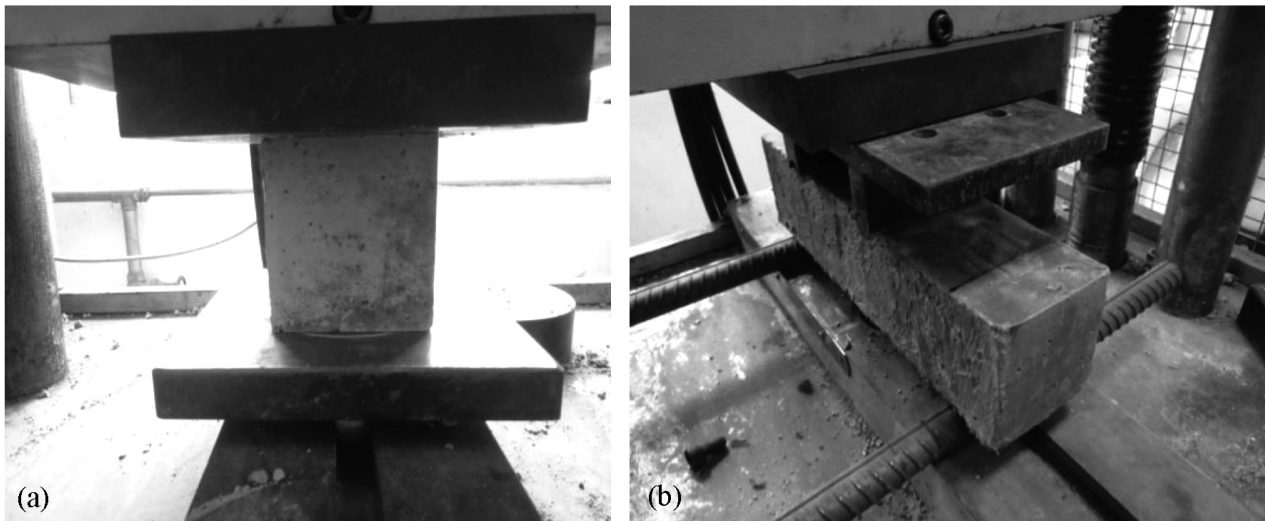


Figure 2: Mechanical test: a) compressive strength test, b) flexural strength test

which is 1.05 for (200×200×200) mm specimen and 0.95 for (100×100×100) mm specimen.

Moreover, when the flexural strength test is performed, the tested specimens are first placed in the center of the bending anti-bending device, as shown in **Figure 2b**, and the smooth surface is used as the bearing surface. The testing machine is started, which should be run at a continuous and equable speed of 0.8–1.0 MPa/s, until the specimen is nearly broken. Record the breaking load and the fracture position of the lower edge of the specimen.

The flexural strength can be obtained as follows:

$$f_f = \frac{Fl}{bh^2} \quad (8)$$

Where  $f_f$  is the flexural strength of the specimen (MPa);  $F$  is the ultimate loading in the flexural test (N);  $l$  is the span between the supports (mm);  $h$  and  $b$  are the height and width, respectively. The compressive and flexural strength results need to be multiplied by 0.95 and 0.85, respectively, which are the conversion factors for the non-standard sizes.

The method for determining the flexural strength value is the same as that for determining the compressive strength value. Moreover, if one of the three specimens has a fracture surface beyond the position of the concentrated loads, the flexural strength of the concrete is calculated based on the test results of the other two specimens. If the difference of the two measured values is no more than 15 % of the smaller measured values, the flexural strength is the average of the two measured values. Otherwise, the test is invalid. If the fracture position of the lower edge of two specimens locates outside the loading line, the test is also invalid.

When the concrete strength grade is less than C60, the strength value of the non-standard specimen should be multiplied by the size conversion factor, which is 0.85 for (100×100×400) mm specimens.

### 3 ANALYSIS AND DISCUSSION

#### 3.1 Compressive strength test

After a standard curing for 1 d and 3 d, the concrete specimens with different fibers were tested to obtain their compressive strengths, which are shown in **Figure 3**.

It can be seen from **Figure 3** that with a total fiber content of 2 %, the compressive strength of the concrete is the minimum when the contents of the steel fiber and PVA fiber are 0.5 % and 1.5 %, respectively, and the compressive strength is the maximum when the content of steel fiber is 2 % (S2P0). In the condition of the maximum steel content is no more than 1.5 %, when the contents of steel fiber and PVA fiber are 1.5 % and 0.12 % (S5P5), the compressive strengths of concrete after a standard curing of 1 d and 3 d are the maximum, with values of 10.23 MPa and 31.52 MPa, respectively.

As shown in **Figure 3**, it is obvious that the fibers have some improvement on the failure forms of the concrete specimens. For the ordinary concrete specimen, during the process of the compressive strength test, one or two micro-cracks occurred firstly on the surface, the initial micro-cracks will expand to other cracks around them. As the load continuously increases, the width of cracks will be expanded gradually, and their number will rapidly increase. This phenomenon remains normal until the cracks distribute in the specimen from top to bottom and the specimen will break into pieces in the end. The failure form of the ordinary concrete specimen is brittle, which means that a brittle failure has occurred. However, the crack expansion processes of the steel fiber and PVA-steel concrete specimens are slow. Although their ultimate strength cannot be improved, the decline rate will be slowed down after the fibers are added. Meanwhile, when the failures of the specimens occur, the fibers try to glue the pieces in a whole cube, which indicates that the specimens have good ductility.

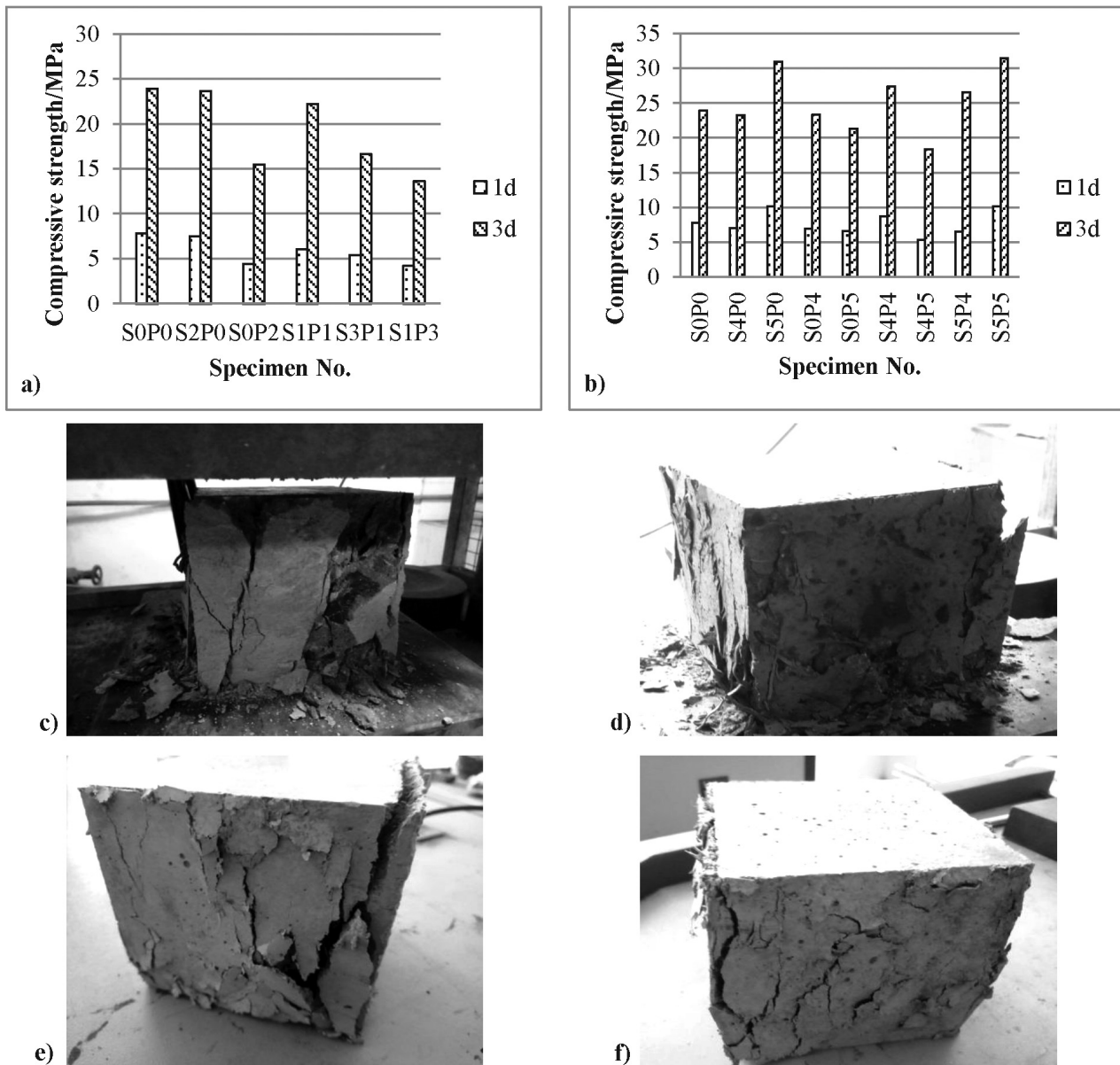


**Figure 3:** Results of compressive test: a) total fiber content is 2 %, b) maximum steel content is no more than 1.5 %, c) failure forms of ordinary concrete, d) failure forms of steel fiber concrete, e) failure forms of PVA fiber concrete, f) failure forms of steel-PVA hybrid fiber concrete

### 3.2 Flexural strength test

After a standard curing of 1 day and 3 days, the concrete specimens with different fiber contents are tested to obtain their flexural strengths, which are shown in **Figure 4**. The appropriate content of PVA and steel fibers will obviously improve the early flexural strength. When the contents of the steel fiber and the PVA fiber are 1.5 % and 0.12 % (S5P5), the flexural strength is the maximum, with the values of 2.08 MPa and 4.48 MPa, respectively.

As shown in **Figure 4**, the ordinary concrete specimen broken directly into two parts in the flexural strength test, which is a brittle failure. However, the specimen with hybrid fibers shows incomplete fracture form due to gluing the fibers in the fracture surface. The

results indicate that the fibers can promote the ductility of the concrete specimens.

### 3.3 Functional mechanism analysis

The results of Section 3.2 indicate that steel fiber, PVA fiber, and steel-PVA hybrid fibers have some positive effects on the early compressive and flexural strengths of the concrete. However, due to the difference of their additive contents, the performances of only several specimens such as S5P0, S4P4, S5P4 and S5P5 for compressive strength test and S2P0, S5P0, S0P4, S0P5, S4P4, S5P4 and S5P5 for flexural strength test are improved, and the improvement degree of flexural strength is 81.3 %, better than that of that of the compressive strength, which is 30.9 %.

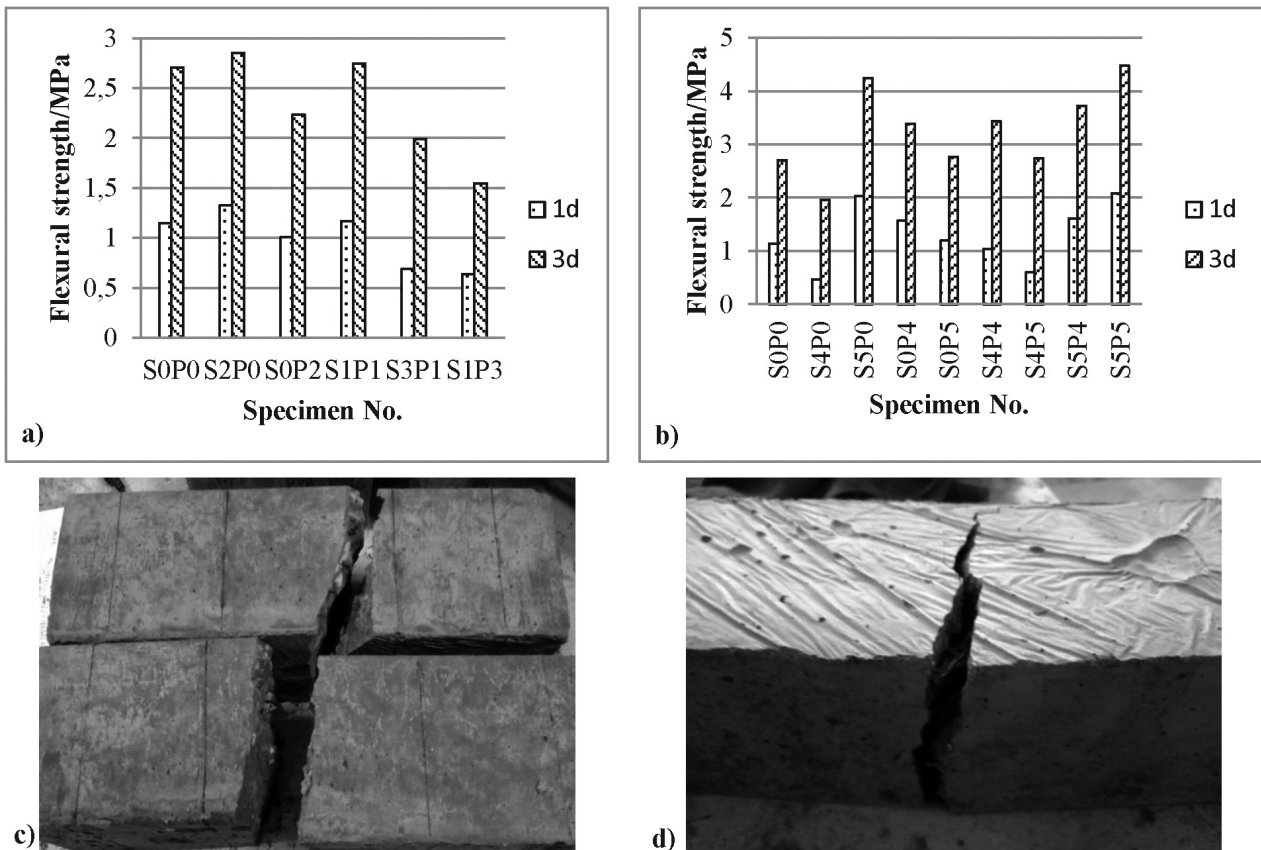


Figure 4: Results of flexural strength test: a) total fiber content is 2 %, b) maximum steel content is no more than 1.5 %. c) failure form of ordinary concrete, d) failure form of steel-PVA hybrid fiber concrete

The main reason for the enhancement mechanism of hybrid fiber concrete is that the PVA fiber has good compatibility with cement, which can form cohesion between the PVA fiber and the cement. At the same time, the PVA fiber can absorb the cracking energy, which means it can inhibit the micro cracks inside the specimen and slow down the expansion of the initial cracks. This mechanism delays the failure and promotes the overall ductility of the concrete specimen.

Furthermore, the PVA fiber has good performance of water absorbing, which can prevent the evaporation of water. This characteristic, as a key factor, is important in the period of concrete curing. And the hydration process of the cement will generate many hydrated products attached to the surface of the PVA fiber, which is combined with the characteristic to further reduce the water loss. Additionally, steel fiber, as a high-strength material, is added in the concrete, which can prevent the brittle failure in the situation of micro and macro cracks, it can be utilized to promote the overall strength.

#### 4 FINITE-ELEMENT ANALYSIS AND CASE STUDY

##### 4.1 Finite-element analysis of the concrete in the anchorage zone

###### 4.1.1 Load

According to the Chinese standard specification CJJ 11-2011,<sup>31</sup> the maximum axle load of Highway Load-I is applied to the finite-element model, where  $G = 140 \times 10^3$  N. And its application areas are four rectangles of 0.2 m  $\times$  0.6 m. The pressure can be obtained as follows:

$$p = \frac{G}{A} = \frac{140 \times 10^3}{0.6 \times 0.2 \times 2} = 0.58 \text{ MPa} \quad (9)$$

where  $G$  and  $A$  are the axle load and application area, respectively.

There are four different loading locations, which are along the longitudinal direction and considered to study the strength performance of the anchorage zone concrete (Figure 5):

1) Location 1: The front edges of the first two wheel tracks are next to the interface between bridge deck pavement and anchorage zone concrete;

2) Location 2: The center lines of the first two wheel tracks coincide with the interface between bridge deck pavement and anchorage zone concrete;

(3) Location 3: The back edges of the first two wheel tracks are next to the interface between bridge deck pavement and anchorage zone concrete;

4) Location 4: The center lines of the first two wheel tracks coincide with the center lines of anchorage zone.

Moreover, the situations of overweight and emergency braking have been considered as another two important factors that influence the stress in the area. For overweight, its range of variations is 21.7 % and 37.9 % based on the max axle load of Highway Loading Grade I. Meanwhile, the emergency braking is converted to a horizontal braking force, which is 0 for a motionless vehicle, 0.10 for the motion in a constant speed, 0.25 for the slow braking and 0.50 for emergency acceleration or braking.<sup>32</sup>

4.1.2 Model parameters

The local finite-element model and its parameters are shown in Figure 6 and Table 2, where the elastic modulus of the C50 concrete for 3 d is calculated according to Equation (10).<sup>33</sup> The Cartesian coordinate is adopted in the finite-element model, where X-direction is the vehicle driving direction (longitudinal direction), Y-direction is the depth direction of the pavement and the Z-direction

is the transverse direction of the pavement (transverse direction). And the boundary condition is that the displacement constraints of three directions are applied on the bottom of the bridge deck.

$$\begin{cases} E(t) = \frac{t}{a_e + b_e \cdot t} \cdot E_{28} \\ a_e = 1.2992 + 82733.13 \cdot e^{-0.3611 E_{28}} \\ b_e = 0.6752 + 0.00738 E_{28} \end{cases} \quad (10)$$

where  $E(t)$  is the elastic modulus of the concrete at  $t$  days (GPa),  $t$  is the time (days),  $E_{28}$  is the elastic modulus of the concrete at 28 d, which is 3.45 GPa according to the Chinese standard specification GB 50010-2010<sup>34</sup> and  $a_e$  and  $b_e$  are the statistical parameters, respectively.

Table 2: Material parameters of finite-element model

Item	Material	Elastic modulus /MPa	Poisson's ratio
Bridge deck pavement	Asphalt concrete	3000	0.35
Bridge slab	Cement concrete	30000	0.25
Anchorage zone concrete	C50 concrete (3d)	23470	0.20

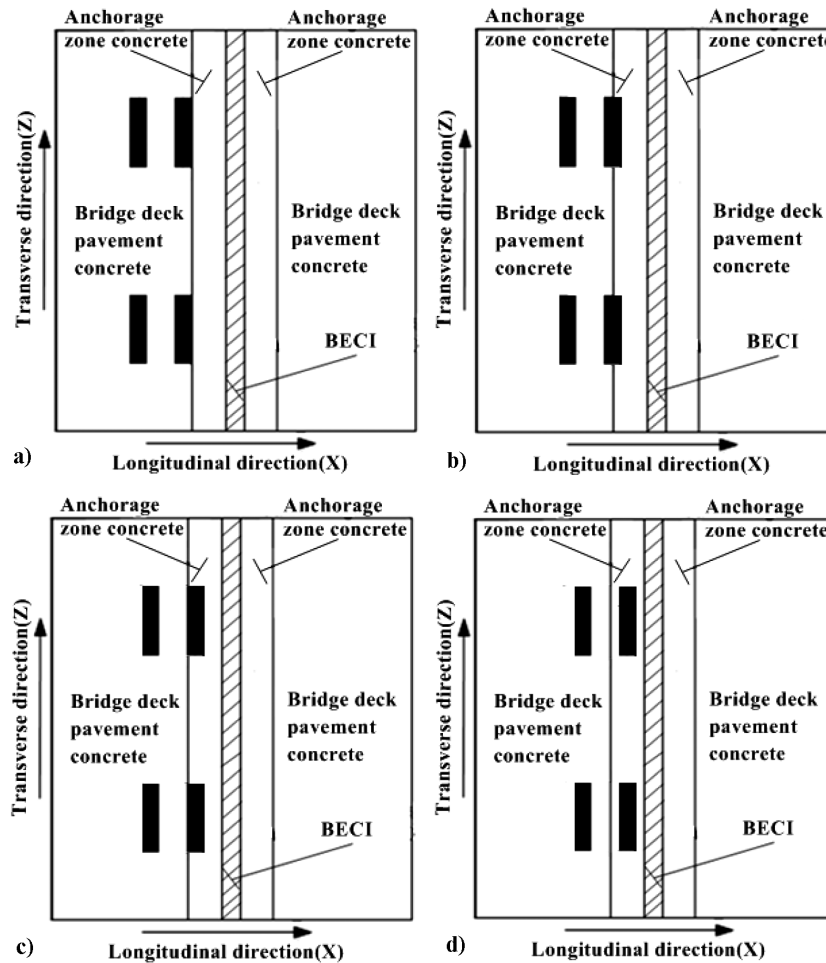


Figure 5: Loading location: a) location 1, b) location 2, c) location 3, d) location 4

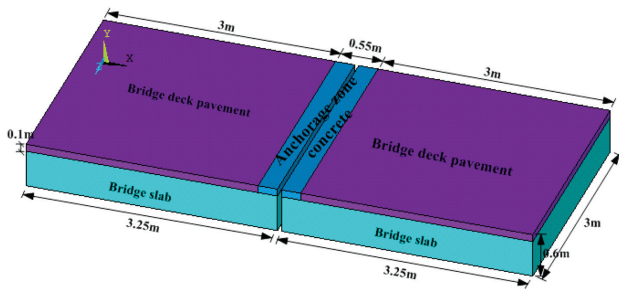


Figure 6: Finite-element model of the BECI of Jihe Bridge

In order to simplify the complexity of the model, some basic assumptions are proposed in <sup>35</sup>:

- 1) The effects of gravity, the negative bending moment of the bridge deck and bridge vibration are all ignored;
- 2) all materials satisfactorily meet relevant standards and requirements;
- 3) the interface between the bridge deck pavement and anchorage zone is simulated by contact element instead of the mechanical connection, and the other components are fixed with each other.

Moreover, the anchorage zone, bridge deck, and bridge deck pavement are all simulated by Solid45, the interface between the bridge deck pavement and anchorage zone is simulated by Conta173 and Targe170. The meshed finite-element model is shown in Figure 7.

4.1.3 Discussion of finite-element analysis

To determine the loading location of maximum stress, the stress data of interface between bridge deck pavement and anchorage zone concrete have been extracted along the longitudinal direction of the bridge deck. The maximum shear and compressive stresses are listed in Table 3.

Table 3: Maximum of shear and compressive stress at four loading locations

Loading location	$\sigma_X$ /MPa	$\sigma_Y$ /MPa	$\sigma_Z$ /MPa	$\tau_{XY}$ /MPa	$\tau_{XZ}$ /MPa	$\tau_{YZ}$ /MPa
1	0.212	0.376	0.159	0.121	0.067	0.069
2	0.203	0.680	0.252	0.072	0.071	0.123
3	0.119	0.376	0.168	0.093	0.030	0.057
4	0.010	0.154	0.062	0.068	0.053	0.018

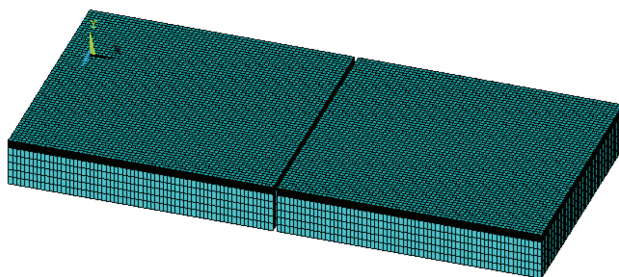
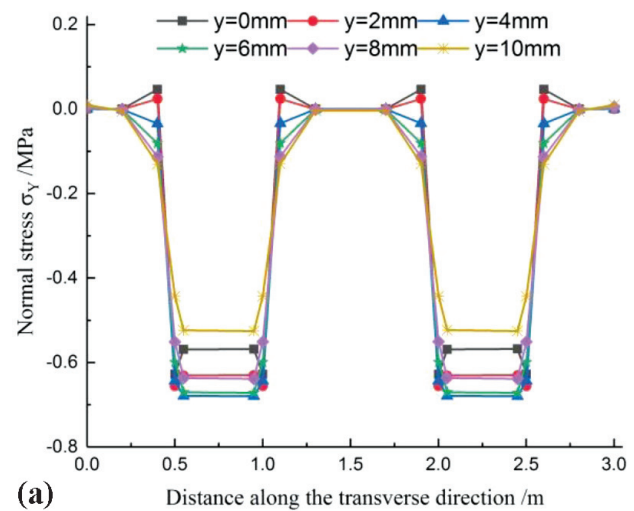


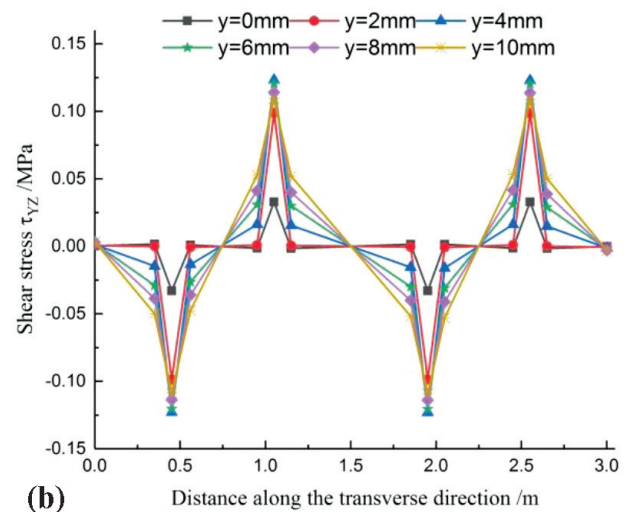
Figure 7: Meshed finite-element model

As listed in Table 3, compared to the others, there is an obvious change for  $\sigma_X$  and  $\tau_{YZ}$  in loading location 2, so loading location 2 and its stress distribution (Y-direction and YZ-direction) can be determined to study the road performance of the steel-PVA hybrid fiber concrete. Therefore, the stress distributions of the interface along the transverse direction (Z) are shown in Figure 8.

Figure 8 indicates that the normal stress  $\sigma_Y$  is in the applying load area of the wheel tracks, and the maximum normal stress occurs at a depth of 4 mm from the bridge deck. For the depth in the range of 0–4 cm, the normal stress of the wheel outside is tensile. Meanwhile, there is an increasing trend for the normal stress in applying the load area. But normal stress of the wheel outside is compressive in the depth of 4–10 cm, while the trend for the normal stress in the applying load area is declined. Moreover, for the shear stress  $\tau_{YZ}$ , one can conclude that the shear stress around the wheel is greater than other locations, its maximum can be obtained at the outside of the wheels. When the depth is in a range of 0–4 cm and



(a)



(b)

Figure 8: Interface stresses along the transverse direction (Z): a) normal stress, b) shears tess  $\tau_{YZ}$

4–10 cm, the shear stress at the outside of the wheels are increasing and decreasing, respectively, which are mainly affected by the vehicle weight and reaction force of bridge slab.

In the following, as an important factor, the overweight, is also considered in this study. The overload coefficients can be determined as 21.7 % and 37.9 %, and their calculated loads are 0.706 MPa and 0.800 MPa. The maximum stresses under different overload levels are listed in **Table 4**.

**Table 4:** Maximum stresses under different overload levels

Loading value /MPa	Compressive stress /MPa	Shear stress /MPa
0.580	0.680	0.123
0.706	0.827	0.150
0.800	0.938	0.170

From **Table 4**, there is a positive relationship between the maximum normal and shear stress under different overload levels. Meanwhile, under the overload level of 37.9 %, the maximum normal stress and shear stress are far less than the ultimate stresses of the concrete after 3-day standard curing, which means the vehicle load cannot cause an overload damage to the anchorage zone concrete. Hence, the mechanical properties of the steel-PVA hybrid fiber concrete are better than that of the ordinary C50 concrete, which means the former is more difficult to destroy under the same loading conditions. Although the elastic modulus of the hybrid fiber concrete cannot be quantified accurately, the mechanical analysis of the C50 concrete provides a powerful and creditable proof to ensure the better road performance in anchorage zone concrete.

In addition, the braking of vehicles can cause damage and separation of the interface between bridge deck pavement and concrete in the anchorage zone; therefore, based on the applied standard values of 0.58 MPa, the vehicle braking is converted to a horizontal force to obtain the maximum stresses, which are listed in **Table 5**.

**Table 5:** Maximum stresses under different horizontal force coefficients

Horizontal force coefficient	Compressive stress /MPa	Shear stress /MPa
0	0.680	0.123
0.10	1.396	0.368
0.25	2.730	0.948
0.50	5.170	1.947

It can be seen from **Table 5** that the maximum compressive and shear stresses increase with the horizontal force coefficients. It is implied that there is a great influence of the horizontal force coefficient on the interface stress. When the horizontal force coefficient changes from 0 to 0.10, the compressive and shear stress will increase by 105.3 % and 199.2 %, respectively. As the coefficient reaches 0.25, the stress increases rapidly and the

change of the shear stress is more obvious. And for the maximum coefficient of 0.50, the maximum shear stress is 1.947 MPa, which is still less than the flexural strength of the steel-PVA hybrid fiber concrete. In the final analysis, there is a good capability of the improved concrete to resist the shear stress generated by the emergency braking of vehicles, which can satisfactorily meet the requirements of early high strength for the anchorage zone concrete.

#### 4.2 Application example

In order to evaluate the road performance of the hybrid fiber concrete, the concrete is used for the anchorage zone of the Jihe Bridge, which is located in the city of Fuyang, Anhui province, China. The experimental compressive strengths are shown in **Table 6**.

**Table 6:** Experimental compressive strengths of steel-PVA hybrid fiber concrete under different curing stages

Concrete	1 d /MPa	3 d /MPa	28 d /MPa
Steel-PVA hybrid fiber concrete	18.7	36.9	50.9
Steel fiber concrete (C50)	10.9	42.1	53.7

The results of **Table 6** indicate that the site experimental compressive strengths of the hybrid fiber concrete after 1 d and 3 d curing are both higher than the results in the lab. And comparing to the C50 concrete, the



**Figure 9:** BECI of the Jihe Bridge using the steel-PVA hybrid fiber concrete

strength of steel-PVA hybrid fiber concrete is better in the condition of 1-day curing than for a steam curing of 48 h, but slightly lower in the condition of 3 d and 28 d. The measured results imply that although the compressive strength of the improved concrete has slightly lower, its early strength is very suitable for the quick construction of the anchorage zone concrete, which can reduce the period of closed traffic and improve the durability of anchorage zone concrete.

As shown in **Figure 9**, the steel-PVA hybrid fiber concrete was utilized in the expansion and contraction installations' anchorage zone of the bridge for about 1 year, which is verified by the regular traffic flow. The new concrete without any damage has good road performance, the improvement of concrete is useful and successful.

## 5 CONCLUSIONS

In this paper, an improved steel-PVA hybrid fiber concrete with high early strength is proposed and constructed by adding steel and PVA fiber in the ordinary concrete. The comprehensive test design method is adopted to evaluate and analyze the mechanical properties of concrete by adding a single steel fiber, single PVA fiber, and hybrid fiber. After 1 d and 3 d of standard curing, the mechanical performances, such as compressive strength and flexural strength, are obtained by compressive and flexural tests in the laboratory. Additionally, the function mechanism of the steel-PVA fiber is discussed. Further, the finite-element model of the anchorage zone concrete is established to compare the road performance of the ordinary concrete and the improved concrete, and the maximum stress loading location is determined to evaluate the effects to anchorage zone concrete. Meanwhile, some factors such as the overload and horizontal coefficient are also considered. The maximum shear and compressive stress are extracted, which are compared with the ultimate stress of steel-PVA hybrid fiber concrete. Eventually, an application example is introduced to verify the practical road performance of the improved concrete. The conclusions can be summarized as follows:

1) PVA fiber and steel fiber additives have a negative effect on the early compressive strength of ordinary concrete. However, PVA fiber is more sensitive to the strength reduction. And for the flexural strength, PVA, steel and steel-PVA hybrid fiber both have some enhancement to ordinary concrete. The optimum added percentages of the fiber additives are 1.5 % for steel and 0.12 % for PVA.

2) The ordinary concrete has significant brittleness. However, due to the fiber glued in the fracture surface, the improved concrete has good ductility and can slow down the destruction process of the concrete specimen.

3) From the results of the finite-element analysis, it is shown that the maximum stresses in the condition of

37.9 % overload and 0.5 horizontal coefficients are less than the ultimate test stress of 3 days curing of ordinary concrete C50. As the early mechanical performances of the steel-PVA hybrid fiber concrete are better than that of ordinary concrete C50. The improved concrete shows good performances of high early strength and ductility, which satisfactorily meet the principle of quick traffic-opening and shorten the repair period of expansion and contraction installations.

4) Through the case study, it is found that the early compressive strength of the steel-PVA hybrid fiber concrete is improved, but the strength after 28 d of standard curing decreased. The proposed steel-PVA hybrid fiber concrete has good ductility and its basic mechanical performance can be ensured. Compared to the ordinary concrete, although there is some reduction in the compressive strength, the improved concrete is very suitable for the quick repair requirements of the anchorage zone, which can reduce the period of closed traffic and show good practical application performance.

## Acknowledgement

The authors gratefully acknowledge that this study was supported by the Science and Technology Progress Project in Transportation (2017), Anhui Province, China (Study on Rapid Replacement of Highway Bridge Expansion Joint Device).

## 6 REFERENCES

- <sup>1</sup> J. P. Romualdi, G. B. Baston, Mechanics of Crack Arrest in Concrete, *J. Eng. Mech.*, 89 (1963) 3, 147–169
- <sup>2</sup> J. P. Romualdi, J. A. Mandel, Tensile strength of concrete affected by uniformly distributed closely spaced short lengths of wire reinforcements, *Am. Concr. Inst., J.*, 61 (1964) 3, 657–672, doi:10.14359/7801
- <sup>3</sup> M. H. Cheyrezy, P. Richard, Reactive powder concretes with high ductility and 200–800 MPa compressive strength, *Am. Concr. Inst. Mater. J.*, 144 (1994) 3, 507–518, doi:10.14359/4536
- <sup>4</sup> J. Zhang, Y. Zhao, The mechanical properties and microstructure of ultra-high-performance concrete containing various supplementary cementitious materials, *J. Sustainable Cem.-Based Mater.*, 6 (2017) 4, 254–266, doi:10.1080/21650373.2016.1262798
- <sup>5</sup> C. J. Shi, Z. M. Wu, J. F. Xiao, D. H. Wang, Z. Y. Huang, Z. Fang, A review on ultra high performance concrete: Part I. Raw materials and mixture design, *Constr. Build. Mater.*, 101 (2015), 741–751, doi:10.1016/j.conbuildmat.2015.10.088
- <sup>6</sup> S. Wang, V. C. Li, Polyvinyl alcohol fiber reinforced engineered cementitious composites: material design and performances, Proceedings of International RILEM workshop on HPFRCC in structural applications, May 23–26, 2005, Honolulu, HI, USA. Bagnoux France: RILEM SARL, 65–73
- <sup>7</sup> Z. M. Wu, C. J. Shi, K. H. Khayat, Effects of different nanomaterials on hardening and performance of ultra-high strength concrete (UHSC), *S. Wan, Cem. Concr. Compos.*, 70 (2016), 24–34, doi:10.1016/j.cemconcomp.2016.03.003
- <sup>8</sup> S. H. Park, D. J. Kim, G. S. Ryu, K. T. Kon, Tensile behavior of ultra high performance hybrid fiber reinforced concrete, *Cem. Concr. Compos.*, 34 (2012) 2, 172–184, doi:10.1016/j.cemconcomp.2011.09.009

- <sup>9</sup> K. Habel, P. Gauvreau, Response of ultra-high performance fiber reinforced concrete (UHPFRC) to impact and static loading, *Cem. Concr. Compos.*, 30 (2008) 10, 938–946, doi:10.1016/j.cemconcomp.2008.09.001
- <sup>10</sup> G. D. Xu, S. Magnani, D. J. Hannant, Tensile behavior of fiber-cement hybrid composites containing polyvinyl alcohol fiber yarns, *Am. Concr. Inst. Mater. J.*, 95 (1998) 6, 667–674, doi:10.14359/409
- <sup>11</sup> V. C. Li, Large volume, high-performance applications of fibers in civil engineering, *J. Appl. Polym. Sci.*, 93 (2002) 3, 83, 660–686, doi:10.1002/app.2263
- <sup>12</sup> V. C. Li, S. Wang, C. Wu, Tensile strain-hardening behavior of polyvinyl alcohol engineered cementitious composite (PVA-ECC), *Am. Concr. Inst. Mater. J.*, 98 (2001) 6, 483–492, doi:10.14359/10851
- <sup>13</sup> J. Zhang, V. C. Li, A. S. Nowak, S. X. Wang, Introducing ductile strip for durability enhancement of concrete slabs, *J. Mater. Civ. Eng.*, 14 (2002) 3, 253–261, doi:10.1061/(ASCE)0899-1561(2002)14:3(253)
- <sup>14</sup> M. Roy, Development and evaluation of high performance fiber reinforced concrete as a repairing material, America, West Virginia University, 2011
- <sup>15</sup> Y. Chen, P. Qiao, Crack growth resistance of hybrid fiber-reinforced cement matrix composites, *Proc. Inst. J. Aerosp. Eng.*, 24 (2011) 2, 154–161, doi:10.1061/(ASCE)AS.1943-5525.0000031
- <sup>16</sup> V. C. Li, C. K. Y. Leung, Steady-state and multiple cracking of short random fiber composites, *ASCE J. Eng. Mech. Div.*, 118 (1992) 11, 2246–2264, doi:10.1061/(asce)0733-9399(1992)118:11(2246)
- <sup>17</sup> P. Soroushian, A. Khan, J. W. Hsu, Mechanical properties of concrete materials reinforced with polypropylene or polyethylene fibers, *Am. Concr. Inst. Mater. J.*, 89 (1992) 6, 535–540, doi:10.14359/4018
- <sup>18</sup> K. Hannawi, H. Bian, W. Prince-Agbodjan, B. Raghavan, Effect of different types of fibers on the microstructure and the mechanical behavior of ultra-high performance fiber-reinforced concretes, *Composites, Part B.*, 86 (2016) 214–220, doi:10.1016/j.compositesb.2015.09.059
- <sup>19</sup> Z. M. Wu, C. J. Shi, W. He, L. M. Wu, Effects of steel fiber content and shape on mechanical properties of ultra high performance concrete, *Constr. Build. Mater.*, 103 (2016) 8–14, doi:10.1016/j.conbuildmat.2015.11.028
- <sup>20</sup> Z. M. Wu, C. J. Shi, W. He, D. H. Wang, Uniaxial compression behavior of ultra-high performance concrete with hybrid steel fiber, *J. Mater. Civ. Eng.*, 28 (2016) 12, 06016017, doi:10.1061/(asce)mt.1943-5533.0001684
- <sup>21</sup> C. D. Atis, O. Karahan, Properties of steel fiber reinforced fly ash concrete, *Constr. Build. Mater.*, 23 (2009) 1, 392–399, doi:10.1016/j.conbuildmat.2007.11.002
- <sup>22</sup> S. F. U. Ahmed, M. Maalej, P. Paramasivam, Flexural responses of hybrid steel–polyethylene fiber reinforced cement composites containing high volume fly ash, *Constr. Build. Mater.*, 21 (2007) 5, 1088–1097, doi:10.1016/j.conbuildmat.2006.01.002
- <sup>23</sup> A. W. Dhawale, G. Moze, Engineered cementitious composites for structural applications, *IJAIEEM*, 2 (2013) 4, 198–205
- <sup>24</sup> V. C. Li, High Performance Fiber Reinforced Cementitious Composites as Durable Material for Concrete Structure Repair, *Int. J. Restor.*, 10 (2004) 2, 163–180, doi:10.1515/rbm-2004-5844
- <sup>25</sup> J. S. Lawler, D. Zampini, S. P. Shah, Permeability of cracked hybrid fiber-reinforced mortar under load, *Am. Concr. Inst. Mater. J.*, 99 (2002) 4, 379–385, doi:10.14359/12220
- <sup>26</sup> JGJ 52-Standard for Technical Requirements and Test Method of Sand and Crushed Stone (Or Gravel) for Ordinary Concrete; Ministry of Construction of the People’s Republic of China: Beijing, China, 2006
- <sup>27</sup> JGJ 63-Standard of Water for Concrete; Ministry of Construction of the People’s Republic of China: Beijing, China, 2006. (In Chinese)
- <sup>28</sup> JGJ 55-General Concrete Mixing Ratio Design Code; Ministry of Housing and Urban-Rural Construction of the People’s Republic of China: Beijing, China, 2011
- <sup>29</sup> CECS 207-High Performance Concrete Application Technical Regulations; Ministry of Construction of the People’s Republic of China: Beijing, China, 2006
- <sup>30</sup> GB/T50081-Standard for test method of mechanical properties on ordinary concrete; Ministry of Construction of the People’s Republic of China: Beijing, China, 2003
- <sup>31</sup> CJJ 11-Code for Design of the Municipal Bridge; Ministry of Housing and Urban-Rural Construction of the People’s Republic of China: Beijing, China, 2011
- <sup>32</sup> R. Friedl, I. Mangerig, Dynamic Amplification of Bridge-Expansion-Joints considering Roughness induced Vehicle Vibrations, *Procedia Eng.*, 199 (2017) 2651–2656, doi:10.1016/j.proeng.2017.09.515
- <sup>33</sup> D. X. Zhang, W. J. Yang, The Experimental Study of Early-Age Strength and Elastic Modulus of Concrete, *Adv. Mater. Res.*, 163–167 (2010) 1192–1197, doi:10.4028/www.scientific.net/AMR.163-167.1192
- <sup>34</sup> GB 50010-Code for design of concrete structures; Ministry of Housing and Urban-Rural Construction of the People’s Republic of China: Beijing, China, 2010
- <sup>35</sup> I. D. Johnson, S. P. McAndrew, McAndrew S P, Research into the condition and performance of bridge deck expansion joints, Crowthorne, Berkshire Transport Research Laboratory, 1993